Michal PĚNIČKA, HOFFMAN Pavel, FOŘT Ivan
Department of Process Engineering
Czech Technical University in Prague

Fluidized bed drying of adhesive particles

Summary

This article is dedicated to the fluidized bed of spherical particles of ion exchangers with a mechanically stirred layer in a batch mode. The essay is to prove a positive impact of mechanical stirring of a fluidized bed on the total drying period and to design parameters of the stirrer (the shape, dimensions, speed, etc.) for uniformed disruption of particle clusters that are formed in the initial stage of the drying process and to provide a conclusive verification of the process on the first and second sphere of the drying kinetics. The objective is thus evaluation of the mechanical stirring effect on the investigated drying process. The performed measurements and calculations suggest that application of the proposed stirring mechanism can shorten drying of ion exchangers by up to 50% in contrast with the original design without a stirrer; the calculation results have confirmed the anticipated process of drying the tested particles in the first drying stage.

Key words: *fluidized bed drying, stirring, mechanical disruption, drying kinetics, first stage of drying*

Suszenie w złożu fluidalnym cząstek adhezyjnych

Streszczenie

Artykuł poświęcony jest procesowi suszenia kulistych cząstek jonowymiennych w złożu fluidalnym, przy wykorzystaniu mieszania mechanicznego w trybie okresowym. Podjęto próbę udowodnienia pozytywnego wpływu mieszania mechanicznego w złożu fluidalnym na całkowity czas mieszania. Zaprojektowano również parametry mieszadła (kształt, wymiary, prędkość, itp.) dla skupisk cząstek wytworzonych w początkowym okresie suszenia. Przeprowadzono kontrolę kinetyki suszenia w pierwszym i drugim okresie suszenia. Celem pracy była ocena wpływu mieszania mechanicznego na badany proces suszenia. Przeprowadzone pomiary i obliczenia sugerują, że zastosowanie zaproponowanego mechanizmu mieszania może z powodzeniem skrócić o 50 % czas mieszania cząstek jonowymiennych w przeciwieństwie do tradycyjnego kształtu bez mieszadła. Wyniki obliczeń potwierdzają przewidywany proces suszenia badanych cząstek w pierwszym etapie suszenia.

Słowa kluczowe: *fluidized bed drying, stirring, mechanical disruption, drying kinetics, first stage of drying*

Nomenclature:

A_S	*Particle surface area, [m²]*
C_{8-13}	*Coefficients*
d	*Diameter, [mm]*
D_{AW}	*Diffusion coefficient, [m² · s⁻¹]*
D_k	*Drying chamber diameter, [mm]*
F	*Mass transfer coefficient, [m · s⁻¹]*
h	*Stirrer width, [mm]*
h_0	*Stirrer aperture size, [mm]*
h_m	*Stirrer height, [mm]*
h_{par}	*Height of fluid layer in rest condition, [mm]*
$h_{par,fl.}$	*Height of fluid layer in fluidization, [mm]*
K	*Mass transfer coefficient, [kg · m⁻² · s⁻¹]*
k, q	*Constants*
m	*Weight, [kg]*
M	*Molecular weight, [kmol · kg⁻¹]*
n	*Number of elements*
N_W	*Drying speed, [kg · m⁻² · s⁻¹]*
$\overline{N_W}$	*Average value of drying speed, [kg · m⁻² · s⁻¹]*
P	*Atmospheric pressure, [Pa]*
p''	*Partial pressure of saturated steam, [Pa]*
Re	*Reynolds number*
s	*Standard deviation*
Sc	*Schmidt number*
Sh	*Sherwood number*
t	*Drying time, [s]*
$\overline{u}$	*Average off–layer speed, [m · s⁻¹]*
u_∞	*Off–layer speed, [m · s⁻¹]*
V	*Relative standard deviation, [%]*
X	*Moisture content of particles, [g_{H2O} · g^{-1}], (d.b.)*
Y_A	*Absolute humidity of outlet air [g_{H2O} · g^{-1}], (dry air)*
Y_W	*Absolute humidity of air on the surface of particles, [g_{H2O} · $g_{d.a.}^{-1}$]*
β	*Mass transfer coefficient, [m² · s⁻¹]*
δ	*Relative error, [%]*
ε	*Porosity*
ε_0	*Porosity in unlimited layer*
φ, γ	*Calculation coefficients*
φ_A	*Average relative moisture, [%]*
μ	*Dynamic viscosity, [Pa · s]*
ν	*Kinetic viscosity, [m² · s⁻¹]*
ρ	*Density, [kg · m⁻³]*

Subscripts

A	*Air*
W	*Water*
SW	*Wet material*
S	*Dry substance*
p	*Particle*
m	*Stirrer*

Introduction

Drying is an energetically very demanding process. It is a sphere where we can find reserves at the time of high prices for energy and the ensuing pressure to reduce them. This article is dedicated to searching for reserves in fluid drying of particles in a batch mode. The particles are very sticky due to the surface tension of the liquid which covers them; the water cannot be removed by a different drying method such as for example centrifuging.

Fluid drying is a type of a drying process with a very intensive transfer of heat and substance between the dried particle and flowing air in which the particles are in a fluid condition. The surface tension of the liquid, which covers the dried particle at the start of the drying process, produces strong stickiness on the particles between each other and the walls of the drying chamber. The batch mode of this process and the small amount of the dried material in one batch prevents application of a vibro–fluid dryer, because these dryers are usually designed for a continuous process. This situation can be solved by drying with a stirred fluid layer, where the stirring process continuously disrupts the clusters of particles and wipes particles stuck to the drying chamber walls.

Process of fluid drying of wet ion exchanger particles

The maximum temperature at which spherical particles of the ion exchanger can be dried is 120°C. The first eighty minutes of drying 350 [g] of the tested amount creates a compact cluster of particles produced by surface tension of water, which covers their surface at the start of the drying. This means that from the start, the drying process proceeds without transition to the fluid condition. Fluidization occurs after eighty minutes of drying. The period from the 80th to the 104th minute is the constant–rate period of drying which is characterized by constant decrease of moisture from the particles in relation to time. After 104 minutes of the drying process, the drying into the falling–rate period of drying in fluidized bed with decreasing speed of moisture removal from the particles.

Material and methods

Spherical particles of ion exchanger

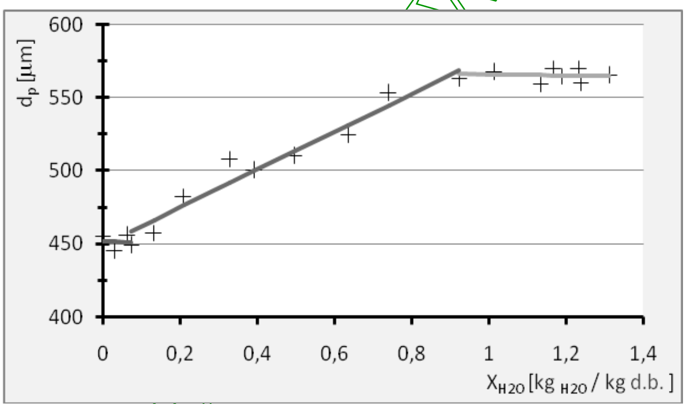

Fig. 1. Dependence of the particle diameter on the moisture content of particles

Rys. 1. Zależności średnicy cząsteczek i ich wilgotności

Spherical particles of ion exchange (cation exchanger and anion exchanger) were selected as a model material. This material is used in processes of nuclear power production and membrane treatment of waste water. Ion exchangers are usually synthetic high–molecular organic substances based on styrene, polyacrylate, phenol formaldehyde resin, etc. We used Marathon – A cation exchanger shaped as spherical particles 450 – 550 [m] in diameter as a model material. This material is peculiar for its volume expansion, which depends on the amount of moisture in the material (Fig. 1.).

Types of stirrers

As mentioned above, the main difficulty of this problem is the initial phase of the drying process, where the particles stick to each other or to the walls because of the surface tension of liquid on the surface and inside the particle. The main task is thus specification of suitable properties of the stirrer. The stirrer must be able to break clusters of the dried particles and wipe the particles off the walls so effectively that the initial drying phase with sticky particles is minimized and the particles are not broken.

To pinpoint the course of the drying process, we developed experimental equipment for the fluidized bed drying with a stirred layer. The experimental equipment is illustrated in Fig. 2. Pressurized air of a known temperature and humidity (point 0 in Fig. 3 is brought from a central air distributor. The air flow is controlled by a control valve and measured with a rotational flowmeter. The air behind the flowmeter is heated by a heater by resistance wires manually controlled by a transformer (point 1 in Fig. 3). The temperature of the heated air is measured before the fluid chamber with a contact thermometer. The humidity of the heated air is determined by the *h*–*x* diagram (Chyský 1977) (Fig. 3), which is valid if the absolute humidity of the drying air is constant, i.e. $Y_{A0} = Y_{A1}$.

A U–manometer is installed at the fluid chamber inlet for monitoring loss of pressure in the fluid bed. The fluid chamber is a glass cylinder 90 × 570 [mm]. The sensor for measuring humidity and temperature of the drying air is located 300 [mm] above the grid of the fluid chamber (point 2 in Fig. 3). The drive for the stirring unit with adjustable speed is located above the chamber.

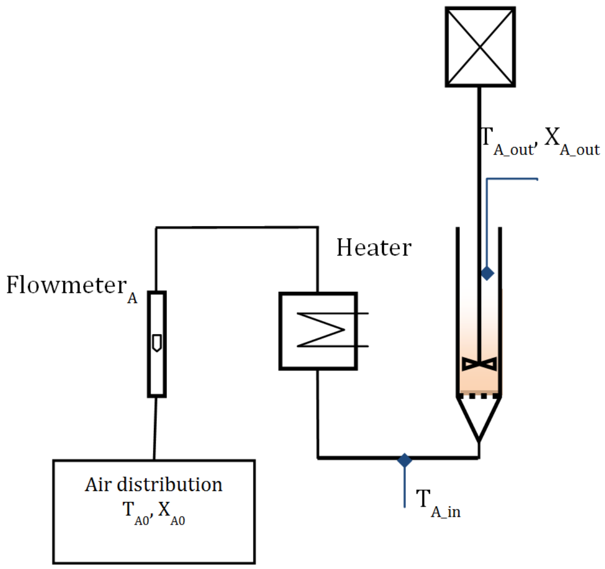

Fig. 2. Scheme of the experimental equipment

Rys. 2. Schemat stanowiska badawczego

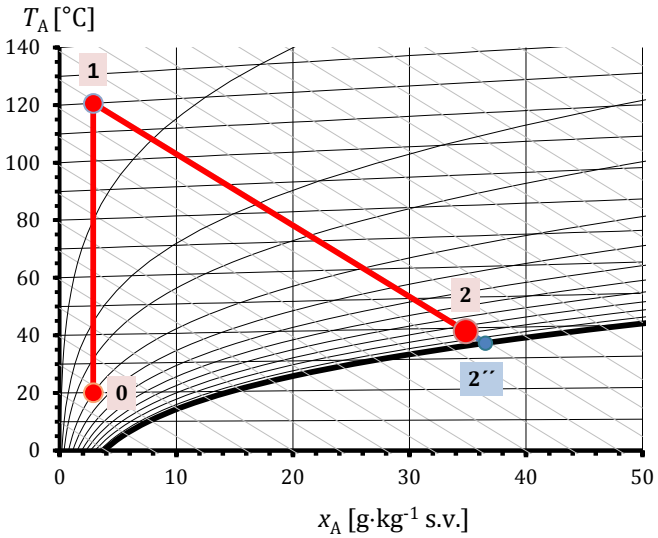

Fig. 3. Mollier's diagram h–x

Rys. 3. Wykres Molliera

Porosity of the dried particles was determined from the relation (1) (Struhár, a Další, 1974)

$$\varepsilon = \varepsilon_0 + 0.33\frac{d_\mathrm{p}}{D_\mathrm{k}} \qquad \textbf{(1)}$$

where ε_0 is porosity in an unlimited layer, which equals 0.39 for spherical particles. The flow of the heated gas behind the heating unit (point 1 in Fig. 3) was determined by a state equation which holds true if the amount of the airflow is constant. The flow in this point determined the off–layer speed of the drying air in the drying chamber. Samples of the dried particles were taken from the centre of the fluid layer on the condition that the particles were ideally stirred, thus the moisture and temperature profile of the fluid layer was homogeneous by action of the stirrer in the initial stage or by a turbulent character of the particles' flow in the fluid condition in the first and second stage of the drying process (Kunii 1991).

Determination of time relation of the drying speed in the first drying period

The stirrer disrupts the forming clusters of particles in the initial drying period, which has a positive impact on the overall drying period. The effect of the stirrer in the first and second periods, when the particles on the surface are sufficiently dry for transition into the fluid condition, may be negative, because the stirrer can disrupt the created fluid layer and the particles will thus not be in ideal contact with the drying air and the transfer effects will be slower. To determine this effect, we must first determine the impact of the volume–shrinkage of the particles (i.e. behavior of the dried particles in the first drying stage) on the drying period. Dependence of the changed particle diameter on the moisture content of particles is illustrated in Fig. 1.

We monitor the spherical ion exchanger particle in its uplift in the fluid dryer, where it is dried in the first drying period, i.e. at a constant drying speed. The drying process of the ion particle is considered if the following simplifying conditions hold true:

1. The dried particles are ideally stirred in the fluid dryer by the drying air.
2. The air's properties (temperature, moisture) do not significantly change during the air flow through the dryer.
3. The change of the ion exchanger particle's volume in the first drying period is caused only by the volume of the dried water evaporated from its surface.

The outcomes of laboratory experiments showed linear dependency of the particle's diameter d_p on its moisture content of particles X_w (Fig. 1), which can be expressed by the relation (2) (Disa 2008):

$$d_\mathrm{p} = X_\mathrm{W}k + q \qquad \textbf{(2)}$$

In the first drying period, the drying speed is determined by a condition where the drying speed is not a feature of time, although the individual values, from which it is composed, are depended on time. This statement is expressed by the relation.

$$N_\mathrm{W} \neq f(t) \qquad \textbf{(3)}$$

where the relation (Mujumdar 1995) is inserted as the drying speed.

$$-\frac{1}{A_\mathrm{s}}\frac{dm_\mathrm{SW}}{d\tau} = \frac{m_\mathrm{S}}{A_\mathrm{s}}\frac{dX_\mathrm{W}}{d\tau} = N_\mathrm{W} \qquad \textbf{(4)}$$

After inserting equation (2) in equation (4), we obtain relation

$$\int_{X_{\mathrm{W}1}}^{X_{\mathrm{W}2}} \frac{dX_\mathrm{W}}{k^2X_\mathrm{W}^2+2kX_\mathrm{W}q+q^2} = -\pi\cdot m_\mathrm{S}\cdot N_\mathrm{w}\int_{t_1}^{t_2} dt \qquad \textbf{(5)}$$

and after the successive integration we obtain equation (6). It describes the relation for the ion exchanger particle's drying speed in the fluid column during the first drying stage, when this value is independent on time t in the interval $t \in \langle t_1; t_2\rangle$ a within its relative moisture $X_\mathrm{W} \in \langle X_{\mathrm{W}1}; X_{\mathrm{W}2}\rangle$:

$$\frac{m_\mathrm{S}\cdot(X_{\mathrm{W}_2}-X_{\mathrm{W}_1})}{\pi\left(q^2+k^2X_{\mathrm{W}_1}X_{\mathrm{W}_2}+kq\left(X_{\mathrm{W}_1}+X_{\mathrm{W}_2}\right)\right)}\frac{1}{(t_2-t_1)} = N_{\mathrm{W}6} \qquad \textbf{(6)}$$

For the necessary verification of the analytic solution in experimental behaviors of the functions, or more precisely, the corresponding interval $t_\mathrm{i} = t_{\mathrm{i}+1} + t_\mathrm{i}$, $d_\mathrm{p} = d_\mathrm{p}(X_\mathrm{W})$ and $X_\mathrm{W} = X_\mathrm{W}(t)$, always for the given interval $X_{\mathrm{w,i}} = X_{\mathrm{W,i}+1} - X_{\mathrm{W,i}}$, the experimental data were used for determination of the particle diameter $d_{\mathrm{p,i}}$ (Fig. 1) and for this diameter of the particle the surface was determined. These values were inserted in equation (7), which produced an estimate of the drying speed in the interval $t \in \langle t_\mathrm{i}; t_{\mathrm{i}+1}\rangle$:

$$-\frac{m_\mathrm{S}}{\pi d_{\mathrm{pi}}^2}\frac{X_{\mathrm{W_i}}-X_{\mathrm{W_{i+1}}}}{t_{\mathrm{i}+1}-t_\mathrm{i}} = N_{\mathrm{Wi}} \qquad \textbf{(7)}$$

The accuracy of the proposed analytical solution (6) was expressed by the difference between the calculated and the measured value of the drying speed expressed by the equation (8) for the standard deviation (9) of the measured drying speed values and the relative standard deviation (10):

$$\delta_{N_W} = \frac{\overline{N_W} - N_{Wi}}{N_{Wi}} \quad (8)$$

$$s_{N_W} = \sqrt{\frac{\sum(N_{Wi} - \overline{N_W})^2}{n-1}} \left[\frac{kg}{m^2 s}\right] \quad (9)$$

$$V_{N_W} = \frac{100\, s_{N_W}}{\overline{N_W}} [\%] \quad (10)$$

and where the average value of the drying speed calculated from the measured data [by equation (7)] is given by the relation (Žitný 2008).

$$\overline{N_W} = \frac{\sum N_{Wi}}{n} \quad (11)$$

Determination of the mass transfer coefficient for the first drying period

The impact of the stirrer on the first drying period can be expressed by the mass transfer coefficient between the stirred and non–stirred layer. This coefficient was determined from the experimental data by equation (12) (Mujumdar 1995), where the K value is the mass transfer coefficient [kg·m^{-2}·s^{-1}].

$$\frac{1}{A_S}\frac{dm_{SW}}{d\tau} = \frac{m_S}{A_S}\frac{d\overline{X}}{d\tau} = K \cdot (Y_W - Y_A) \quad (12)$$

In this equation, Y_W expresses the absolute moisture of the drying air in the boundary layer, which accumulates around the dried particle and Y_A is the absolute moisture of the drying air on the outlet from the dryer. For a potential comparison of the mass transfer coefficient by a criterion equation (14) (Ditl 1996).

$$\beta_{13} = \frac{K}{\rho_A} \quad (13)$$

Analytic determination of the mass transfer coefficient was obtained by a criterion equation (14) (Gupta et al. 1962) and (Ditl 1996) and is valid for the fluid layer:

$$Sh = Re \cdot Sc^{0.33}\left[0.01 + \frac{0.863}{Re^{0.58} - 0.483}\right] = \frac{F \cdot d_p}{D_{AB}} \quad (14)$$

where validity of this relation is for the defined interval 20 < Re < 3000. Here the Reynolds number for the spherical particle is defined as

$$Re = \frac{\overline{u'} \cdot d_p \cdot \rho_A}{\mu_A} \quad (15)$$

where $\overline{u'}$ is the average void speed

$$\overline{u'} = \frac{u_\infty}{\varepsilon} \quad (16)$$

and the density of the moist air as per (Chyský 1977)

$$\rho_A = \frac{1.316 \cdot 10^{-3}}{T_A}(2.65 \cdot p + \varphi_A \cdot p''_V) \quad (17)$$

and the pressure of saturated steam at the pressure T was determined by relation (18) for the temperature range from 0°C to 200°C:

$$lnp''_V = \frac{C_8}{T} + C_9 + C_{10} \cdot T + C_{11} \cdot T^2 + C_{12} \cdot T^3 + C_{13} \cdot \ln(T) \quad (18)$$

The Schmidt number is defined by relation

$$Sc = \frac{\upsilon_A}{D_{AW}} \quad (19)$$

where the diffusion coefficient of air moisture can be calculated by relation (Rossié 1953)

$$D_{AW} = 2.193 \cdot 10^{-6}\left(\frac{1}{p}\right)\left(\frac{T}{273}\right)^{1.80} \quad (20)$$

Here, υ_A is the kinetic viscosity of the dry air at the average temperature and pressure in the dry substance. To be able to compare the mass transfer coefficients F (14) and β_{13} (13), relation (Ditl 1996) was applied

$$\beta_{21} = \frac{F}{\varphi} \quad (21)$$

where

$$\varphi = \frac{x_{A1} - x_{A2}}{ln\frac{\gamma - x_{A2}}{\gamma - x_{A1}}} \quad (22)$$

On condition that it concerns diffusion of moisture absorbed by the layer to the surface of the pore in the open system (Ditl 1996), it holds that

$$\gamma = \frac{1}{1 - \sqrt{\frac{M_A}{M_W}}} \quad (23)$$

The agreement between the mass transfer coefficients β_{13} a β_{21} can be expressed by a relative error according to the equation

$$\delta = \frac{\beta_{13} - \beta_{21}}{\beta_{13}} \quad (24)$$

Results and discussion

Influence of the stirrer's position

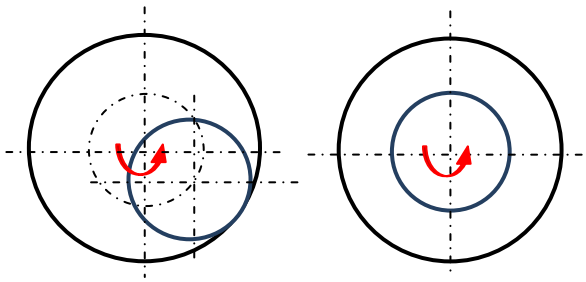

Fig. 4. Eccentric location of the stirrer (A) and centric location of the stirrer (B)
Rys. 4. Niecentralne ułożenie mieszadła (A) Centralne ułożenie mieszadła (B)

A partial task in designing an optimized stirrer concerned its attachment in the drying chamber. We tried two main versions, i.e. an eccentric location (Fig. 4) and a centric location of the stirrer (Fig. 5). The assumptions and subsequent experiments show that the optimized stirrer must be located centrically in the tank and its diameter must be 0.95 – 0.97 of the drying chamber's inner diameter. The bottom edge of the stirrer above the grid should not be higher than 5 [mm]. The

main reason for a centric arrangement is occurrence of undesired vibrations of the whole stirring aggregate, impacts of the stirrer against the chamber walls and a subsequent degradation of the dried material.

The size of the stirrer is determined by a necessity to wipe the stuck material off the walls and homogenization of the entire batch. If the stirrer's diameter is small, a layer of wet material accumulates on the walls of the drying chamber, thus increasing the speed of the drying air above the particle flight velocity. Location of the stirrer immediately above the dryer grate is determined by the thickness of the accumulated layer of the wet material, which blocks access of air into the chamber, thus causing overheating of the material and local increase of the air speed above the particle flight velocity. The dried particles have a strong tendency towards creating a fountain or spurting type of fluid layer, which is not as beneficial for transfer of mass as a laminar or fluid type of layer.

1. Influence of the stirrer speed

The experiments proved a hypothesis that the efficiency to break clusters of particles is not sufficient if the speed is low and the cluster of particles rotates together with the stirrer (Fig. 6). Conversely, if the speed of the stirrer is too high, the stirrer obstructs setting of the fluid layer and constantly disturbs it. This effect affects the drying period in the first and second drying periods, prolonging them 1.2 – 1.8 times in contrast with unstirred condition; this is also true for a low stirrer speed.

2. Design of an optimized stirrer for a minimal drying period

Based on experiments with standardized stirrers, we designed a prototype stirrer called "Wire Stirrer", which is illustrated in Figure 6. The stirrer is made of stainless steel wire 0.4 – 0.6 [mm] in diameters. It is designed for a centric arrangement. The stirrer diameter is 0.95 – 0.97 d/D_k and it is 2.8 – 5 × higher than the rest position of the initial material layer high. The estimated speed is about 50 [min^{-1}], and the peripheral speed of the blade is 0.225 – 0.26 [m·s^{-1}].

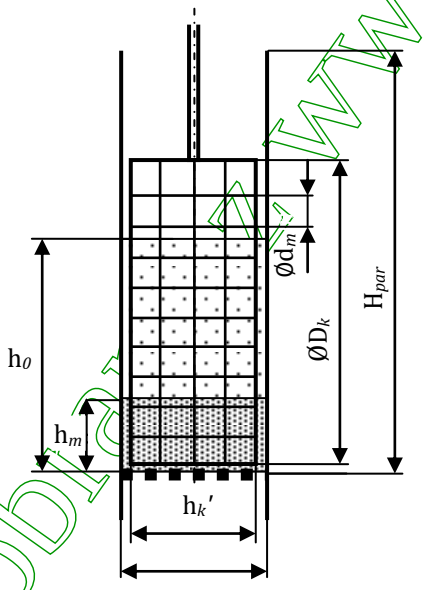

Fig. 5. Scheme of a wire stirrer

Rys. 5. Schemat mieszadła drucianego

We also made experiments with sizes and shapes of apertures in the stirrer. The sizes of square apertures were 2.5 × 2.5 [mm], 10 × 10 [mm] and 25 × 25 [mm]; rectangular apertures were 25 × 2.5 [mm] and 25 × 10 [mm], positioned upright and sideways. The experiments showed that if the apertures are small, the stirrer fails to break a cluster of large particles, which rotates together with the stirrer. If the apertures are too large, the cluster is broken regularly, but only into insufficiently small clusters. The orientation and shape of apertures had no effect on breaking the cluster. The optimum aperture size was specified as 10 × 10 [mm].

Influence on individual periods of the drying process

The drying curves with stirred and unstirred fluid layer are compared in Figure 7. It is clear from this chart that the wire stirrer has the main impact on the initial period of the drying process (full lines in Fig. 7), that is, the particles are stuck. This region is in a range of particles' relative moisture higher than c. 65 – 50% or absolute moisture higher than c. 1 (kg$_{H2O}$/kg d.b.). The particles stick to each other and the walls and do not reach the fluid condition. In a version with a stirred fluid layer, the total drying period of the initial sphere drops from eighty to thirty minutes, i.e. by up to 60%.

It is also clear that the stirrer has no negative impact on the speed of moisture removal from the material in the first and second drying periods where the particles are in the fluid condition (in uplift). The initial conditions in the inlet correspond to the temperature of 120°C and relative air humidity 20% (Fig. 3 point 1).

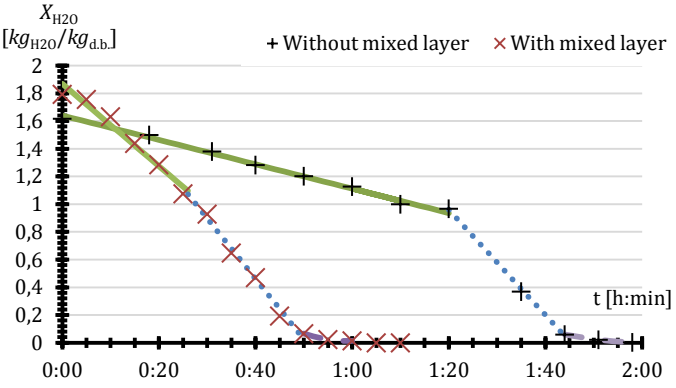

Fig. 6. Comparison of the drying curves

Rys. 6. Porównanie krzywych suszenia

The moisture Y_W was determined (Fig. 3 point 2´´) on condition that the air is fully saturated with water vapours and the surface temperature of the dried particle equals the value of a wet thermometer, i.e. 35.6°C. This temperature was determined by the Mollier diagram (Chyský 1977) Fig. 3 on condition of an isoenthalpic process during the drying, which is illustrated in Figure 3 between points 1 and 2´´. The Y_G moisture corresponded to moisture on the outlet from the dryer, where the outlet temperature was 36.7°C and the moisture 93% as per (Fig. 3 point 2). The numerical expression of the drying speed calculated N_{w6} (6), measured by $\overline{N_W}$ (11) and the relative errors from equation (8), the standard deviations (9) and the relative standard deviations (10) for determination of the drying speed in the first drying period are summarized in Table 1. Table 2 illustrates the mass transfer coefficients for the stirred and the non–stirred layers.

Table 1. Outline of errors when determining the drying speed
Tabela 1. Błędy podczas określania szybkości suszenia

			Stirred layer;	Non – stirred
Drying speed; Szybkość suszenia	N_wBłą	kg·m^{-2}·s^{-1}	1.84·10^{-6}	1.62·10^{-6}
Average drying speed; Średnia szybkość suszenia	$\overline{N_W}$	kg·m^{-2}·s^{-1}	1.51·10^{-6}	1.41·10^{-6}
Relative error; Błąd	δ_{N_W}	%	17.65	13.00
Standard deviation; Odchylenie standardowe	s_{N_W}	kg·m^{-2}·s^{-1}	2.99·10^{-6}	3.08·10^{-6}
Relative standard deviation; Względne odchylenie standardowe	V_{N_W}	%	2.0	2.2

The differences in values determined by experiment, relations adopted from the reference materials (Ditl 1996; Mujumdar 1995) and from theoretical relations (6) are caused by introduction of simplifying conditions of the equation (4), which are mentioned above.

Another source of errors comes from axial and radial non–homogeneity of the temperature field in the fluid chamber, in spite a vigorous stirring of the particles by the turbulent character of the flow in the fluid bed. Determination of the wet bulb temperature by an analytic method can be regarded another source of a total error. The effect of the stirrer on the first drying period is positive, which can be documented by a 13% higher mass transfer coefficient in the stirred layer in contrast to the non–stirred layer (Table 2). The main benefit of the proposed equipment regards the fact that the stirrer does not affect the accumulated fluid layer and wipes the wet particles off the column wall back to the fluid bed, where more intensive transfer processes are produced.

Tabela 2. Zestawienie wartości określanych dla współczynnika przenikania masy
Table 2. Summary of values determined for the mass transfer coefficient

			Stirred layer; Z mieszaniem	Non–stirred layer; Bez mieszania
Porosity; Porowatość	ε		0.85	
Off–layer speed; Szybkość przy warstwie	u_∞	m·s^{-1}	2.5	
Average void speed; Prędkość średnia	$\overline{u}$	m·s^{-1}	2.94	
Particle diameter; Średnica cząstek	d_p	m	5.00E–04	
Surface temperature of particles; Temperatura na powierzchni cząstek	T_W	°C	35	
Average relative moisture of particles; Średnia wilgotność względna cząstek	φ_W	%	99.9	
Specific moisture of particles; Wilgotność cząstek	x_W	g_{H2O}·g^{-1}	0.037	
Air temperature of out; Temperatura powietrza na wyjściu	T_A	°C	38.7	
Average relative moisture; Średnia wilgotność względna	φ_A	%	85.0	
Specific moisture; Wilgotność	x_A	g_{H2O}·g^{-1}	0.038	
Density; Gęstość	ρ_A	kg·m^{-3}	1.155	
Dynamic viscosity; Lepkość dynamiczna	μ_A	Pa·s	19.1E–6	
Kinetic viscosity; Lepkość kinetyczna	ν_A	m^{-2}·s^{-1}	16.6E–6	
Partial pressure of saturated steam; Ciśnienie pary nasyconej	p''_A	Pa	6882	
Diffusion coefficient; współczynnik dyfuzji	D_{AW}	m^{-2}·s^{-1}	34.7E–6	
Reynolds number; liczba Reynoldsa	Re	–	90	
Schmidt number; liczba Schmidta	Sc	–	468.5E–3	
Sherwood number; liczba Sherwooda	Sh	–	5	
Mass transfer coefficient; Współczynnik przenikania masy	F	m·s^{-1}	0.369	
Drying speed; Prędkość suszenia	N_w	kg·m^{-2}·s^{-1}	1.51E–04	1.41E–04
Mass transfer coefficient; Współczynnik przenikania masy	β_Y	kg·m^{-2}·s^{-1}	0.0951	0.0888
Mass transfer coefficient; Współczynnik przenikania masy	β_{21}	m·s^{-1}	0.079	0.079
Mass transfer coefficient; Współczynnik przenikania masy	B_{13}	m·s^{-1}	0.082	0.077
Relative error; Błąd	δ	%	4.8	2.1

Conclusions

W trakcie badań stwierdzono, że dostarczanie dodatkowego ciepła za pomocą promienników podczerwieni znacznie skraca czas sublimacji. Zastosowanie promienników o mocy 10W może skrócić czas procesu o 30%. Czas ten można skrócić jeszcze bardziej, poprzez nastawienie mocy promienników na 50W (70%). Dalsze zwiększenie mocy promienników wpływa w niewielkim stopniu na przyspieszenie procesu sublimacji. Ponadto wyższe nastawy mocy promienników powodują znaczny wzrost temperatury w komorze. Nie jest wskazane przekraczanie temperatury na powierzchni próbki T_p powyżej 20°C oraz temperatury wokół niej T_k powyżej 30°C. Bezpieczne wartości temperatury w komorze osiągnięto dla mocy promienników rzędu 10W.

Acknowledgements

We express our gratitude for the support from grant SGS2012 at ČVUT in Prague (SGS12/057/OHK2/1T/12) and the re-

search program MŠMT ČR (6840770035), which enabled us to make an experimental verification of the drying hypothesis.

References

1. Ditl P. 1996. *Diffusion and Separation Process (in Czech).* Prague: Publishing House of Czech Technical University in Prague.
2. Gupta A. S., Thodos G. 1962. *Mass and heat transfer in the flow of fluids through fixed and fluidized beds of spherical particle.* Houston: AIChE Journal, 8, 608–610.
3. Chyský J. 1977. *The moist air (in Czech).* Prague: Publishing House of Czech Technical University in Prague.
4. Mujumdar A. S. 1995. *Handbook of Industrial Drying.* New York: Dekker.
5. Rossié K. 1953. *Die Diffusion von Wasserdampf in Luft bei Temperaturen bis 300°C.* Frost: Forschung im Ingenieurwesen, 19, 49–58.
6. Struhár L., Hlavačka V. 1974. *Porosity of the particle layers (in Czech).* Prague: ZTV, 17–27.
7. Disa A.O., Desmorieux H. 2008. *Convective drying charakteristics of Amelie mango*. Journal of Food Engineering, 20, 429–437.
8. Kunii D., Levenspiel O. 1991. *Fluidization Engineering*. Stoneham: Butterworth–Heinemann.
9. Žitný R. 2008. *Numerical analysis of the process.* Prague: ČVUT.

Michal Pěnička, Hoffman Pavel, Fořt Ivan
Czech Technical University in Prague,
Department of Process Engineering,
Technická 4, 166 07 Prague,
Czech Republic; Phone No.: +420 224352714,
e–mail: michal.penicka@fs.cvut.cz